

# NONEQUILIBRIUM MOLECULAR DYNAMICS OF CLASSICAL FLUIDS

H. A. POSCH<sup>1</sup> and W. G. HOOVER<sup>2</sup>

<sup>1</sup>*Institute for Experimental Physics  
University of Vienna, Boltzmannngasse 5  
A-1090 Vienna, Austria*

<sup>2</sup>*Department of Applied Science  
University of California at Davis/Livermore and  
Lawrence Livermore National Laboratory, California 94550, USA*

**ABSTRACT.** Nonequilibrium systems in thermodynamic steady states can be studied by computer simulation, and the calculated transport coefficients are in agreement with results obtained by equilibrium methods. The basic algorithms are discussed. Although they require the incorporation of a thermostating procedure, the resulting equations of motion are *time-reversible*. The observed *macroscopic irreversibility* is a consequence of the Lyapunov instability of the system measured by the spectrum of Lyapunov exponents. The phase-space distribution does not remain smooth and well-behaved but collapses onto a multifractal strange attractor in phase space with an information dimension smaller than the phase-space dimension. The attractor even remains fractal if it is projected onto a subspace spanned only by phase-space variables which are not directly affected by the computer thermostat. This is demonstrated for boundary-driven planar Couette flow, for which the number of variables associated with the thermostatted boundary can be made small.

## 1. Macroscopic Transport Coefficients from Microscopic Equations of Motion

The dynamical properties of molecules in liquids and solids are of considerable practical and theoretical interest and have been studied extensively in the past. For systems in thermodynamic equilibrium computer simulations have been proven to be indispensable for an understanding of experimentally determined correlation functions and for providing a link to statistical mechanical theories based on the ensemble theory of Gibbs [1, 2, 3]. Even linear transport coefficients are accessible in this way as has been demonstrated by Green [4] and Kubo [5]. It is a consequence of their (adiabatic) *linear-response theory* that any transport coefficient can be expressed as a time integral of an equilibrium correlation function of the associated dissipative flux  $J$ . The result is the famous Green - Kubo integral [6]

$$L = \beta \int_0^{\infty} dt \langle J(0)J(t) \rangle_0. \quad (1)$$

Here,  $\beta = 1/kT$ ,  $k$  is Boltzmann's constant and  $T$  is the temperature.

However, Alder and Wainwright discovered already in 1967 that highly collective excitations in a fluid [7] seriously impede an efficient evaluation of such integrals. The long-time decay of these correlation functions can be slow and for the velocity autocorrelation functions typically follows a power law  $\sim t^{-d/2}$ , where  $d$  is the space dimension of the system. In two dimensions the respective Green - Kubo integrals diverge logarithmically with system size. In three dimensions the situation is less dramatic since the transport coefficients linear in the applied perturbation do exist, but nonlinear coefficients - such as the nonlinear Burnett coefficients for shear flow - still diverge [8]. An alternative method for the evaluation of transport properties was therefore developed which is much closer in spirit to actual experiments carried out in the laboratory than the fluctuation-dissipation approach mentioned above. This method, known as *nonequilibrium molecular dynamics* (NEMD), was pioneered by W.G.Hoover and W. T. Ashurst [9] and developed further by D.Evans and G.Morriss [10], and many others [11]. It consists in driving the system away from equilibrium and measuring directly the resulting nonequilibrium fluxes from which the transport coefficients may be deduced. To see this we recall that in the *adiabatic* linear response limit the averaged value of this flux at time  $t > 0$  after switching on a possibly time-dependent perturbation  $X(t)$  at time  $t = 0$  is given by

$$\langle J(t) \rangle = -\beta \int_0^t d\tau \langle J(t-\tau)J(0) \rangle_0 X(\tau). \quad (2)$$

For simplicity we assume that the perturbation is constant for positive times,

$$X(t) = X\Theta(t), \quad (3)$$

$\Theta$  being the unit-step function. The more general case of time-varying perturbations has been discussed in refs. [12] and [13]. Then (2) with the help of (1) may be transformed into

$$L = \lim_{X \rightarrow 0} \lim_{t \rightarrow \infty} -\frac{\langle J(t) \rangle}{X}. \quad (4)$$

This forms one basis for the determination of transport coefficients with NEMD. Equivalently, the dissipated heat associated with the nonequilibrium driving can be used to evaluate the transport coefficients [14]. As indicated, either method requires an extrapolation to the limit of vanishing perturbations since the magnitude of  $X$  necessary for the response  $J(t)$  to exceed the numerical noise is orders of magnitude larger than corresponding perturbations attainable in the laboratory. In spite of the extra effort this method is often more efficient than equilibrium techniques [15].

Iacucci, Ciccotti and MacDonald suggested an alternative means for measuring transport coefficients [16]. Their idea was to apply a very small external field, and then to study the additional offset current induced by the field over and above the relatively large equilibrium fluctuations. Though in principle this method is entirely correct, its utility is somewhat limited by the inevitable Lyapunov instability. The instability artificially increases the phase-space offset between the perturbed and unperturbed trajectories, causing the accuracy of the offset-current measurement to deteriorate after a few collision times.

Let us distinguish two types of driving perturbations, *mechanical* and *thermal*. A *mechanical* perturbation can always be written as an external mechanical field acting on the particles' coordinates. It shows up explicitly in the respective expression for the Hamiltonian of the perturbed system and - consequently - in the equations of motion for the

particles. The color field for studying the conductivity of color-charged particles will serve as an example in Section 2. By contrast, the most common phenomena associated with the transport of conserved properties such as linear momentum (viscosity) and heat (thermal conductivity) do not fall into this category. They belong to the second class of *thermally* perturbed systems for which in general no perturbation Hamiltonian can be written down. Instead, fictitious “thermal forces” proportional to the particles’ momenta, in the case of shear viscosity, and to enthalpy, in the case of heat conduction, must be introduced. These thermal forces drive the system away from equilibrium and also show up explicitly in the particles’ equations of motion [10]. For  $t > 0$  they can be written as

$$\dot{\Gamma} = \begin{cases} \dot{\mathbf{q}} &= \mathbf{p}/m + \mathcal{Q}(\mathbf{q}, \mathbf{p})X(t) \\ \dot{\mathbf{p}} &= \mathbf{F}(\mathbf{q}) + \mathcal{P}(\mathbf{q}, \mathbf{p})X(t) - \zeta \mathbf{p} \end{cases} \quad (5)$$

Here,  $\Gamma = (\mathbf{q}, \mathbf{p})$  denotes a point in phase space, where  $\mathbf{q}$  stands for all coordinates, and  $\mathbf{p}$  for the peculiar momenta of the particles.  $\mathbf{F} = -\partial\Phi/\partial\mathbf{q}$  is the intrinsic atomistic force on a particle, and the potential energy  $\Phi(\mathbf{q})$  may also include boundary interactions.  $\mathcal{Q}(\mathbf{q}, \mathbf{p})$  and  $\mathcal{P}(\mathbf{q}, \mathbf{p})$  are vector-valued phase functions which couple the perturbation  $X(t)$  to the system. Although their functional form depends on the transport coefficient in question, they can always be chosen such that an arbitrary phase-volume element  $\delta v$  is a constant of the motion for the adiabatic case, for which  $\zeta \equiv 0$  in (5):

$$\frac{d \ln \delta v}{dt} = \frac{\partial}{\partial \Gamma} \cdot \dot{\Gamma} = \left( \frac{\partial}{\partial \mathbf{q}} \cdot \mathcal{Q} + \frac{\partial}{\partial \mathbf{p}} \cdot \mathcal{P} \right) X = 0. \quad (6)$$

For Hamiltonian systems this condition is always valid. It is assumed in the following that (6) also holds in the non-Hamiltonian case. This simplifies the analysis without serious restrictions. Furthermore,  $X$  is written as a scalar such that any vectorial or tensorial character of the perturbation must be included in the definitions of  $\mathcal{Q}$  and  $\mathcal{P}$ .

The identification of  $\mathbf{p}$  with a peculiar velocity in (5) implies that  $\mathbf{p}/m$  is measured relative to a stationary hydrodynamic streaming velocity  $\mathbf{u}(\mathbf{q})$ . This restricts the applicability of the method to lower-Reynolds number non-turbulent flows [17]. The internal energy is given by

$$H_0 = \sum \frac{\mathbf{p}^2}{2m} + \Phi(\mathbf{q}), \quad (7)$$

and the temperature is defined by

$$\langle K \rangle = \left\langle \sum \frac{\mathbf{p}^2}{2m} \right\rangle = \frac{d}{2}(N-1)kT, \quad (8)$$

where  $d$  is the dimension. The minus-one term comes from the center-of-mass motion which does not contribute to the temperature. In particular applications such as the study of clusters it might well be desirable to remove the rotational contributions as well. Strictly speaking,  $T$  is the thermodynamic temperature only at equilibrium ( $X = 0$ ) and if the averaging is performed with a canonical ensemble. For general non-equilibrium states the distribution of the peculiar momenta is not necessarily Maxwellian [18], and (8) becomes the defining equation of a nonequilibrium kinetic temperature, which may be determined with a small ideal gas thermometer. For nonequilibrium conditions the definition of a thermodynamic temperature,  $T \equiv (\partial E / \partial S)_V$ , is complicated by the singular properties of

Gibbs' nonequilibrium entropy. As will be shown in more detail in Sec. 5, Gibbs' entropy can diverge in nonequilibrium steady states, rendering the entropic definition useless. Rough estimates based on coarse-grained phase-space densities have revealed numbers for such a temperature which are indeed significantly smaller than the kinetic temperature used above [19].

The adiabatic rate of change of the internal energy,

$$\dot{H}_0 = \sum \left( \frac{\partial H_0}{\partial \mathbf{q}} \cdot \dot{\mathbf{q}} + \frac{\partial H_0}{\partial \mathbf{p}} \cdot \dot{\mathbf{p}} \right) \equiv -J(t)X, \quad (9)$$

defines the dissipative flux generated by  $X$ :

$$J(t) = \sum \left( -\mathcal{P} \cdot \frac{\mathbf{p}}{m} + \mathcal{Q} \cdot \mathbf{F} \right). \quad (10)$$

With a constant perturbation acting on the system for positive times, another complication arises: work is continuously performed on the system, which consequently heats up and never reaches a steady state. Because of (2) the rate with which the internal energy increases is of second order in the applied perturbation and has consequently been ignored in the adiabatic linear-response theory leading to (1). It obviously cannot be neglected if the limit  $t \rightarrow \infty$  in (7) is taken seriously. In view of the large perturbations required for NEMD, this excess heat must be removed from the system with a thermostat. This is also common laboratory practice, if an experiment is to be carried out under nonequilibrium steady-state conditions. In the context of a computer simulation this "thermostat" consists of an extra frictional feedback term  $-\zeta(t)\mathbf{p}$  added to the right-hand side of the second of the motion equations (5). Only a single scalar variable  $\zeta$  is required. This represents an external thermostat which in the real world consists of many external degrees of freedom. In this sense  $\zeta$  can be viewed as a general boundary condition to which all thermostatted momenta are subjected. For equilibrium states  $\zeta$  fluctuates around  $\langle \zeta \rangle = 0$ . For stationary nonequilibrium conditions  $\langle \zeta \rangle > 0$  and is nonlinear, quadratic in the current close to equilibrium. To determine  $\zeta$  we require that the equations of motion be invariant with respect to the time-reversal transformation  $\vartheta : (\mathbf{q}, \mathbf{p}, \zeta) \rightarrow (\mathbf{q}, -\mathbf{p}, -\zeta)$ , which reverses the trajectory in phase space. Consequently,  $\zeta$  is treated as a momentum-like variable. This follows from Nosé's original derivation [20]. Two methods are commonly used which differ in the ensemble they generate under equilibrium conditions (for which  $X = 0$ ).

**Gaussian thermostat:** One requires that the peculiar kinetic energy  $K(\mathbf{p}) = \sum \mathbf{p}^2/2m$  be a constant of the motion,  $K_0$ . This non-holonomic constraint may be fulfilled by adding a constraining force to the momentum equations of motion [21, 22, 10]. Following a prescription of Gauss [23] this force is minimized in the least-squares sense, which leads to the term  $-\zeta\mathbf{p}$  in the second of the equations (5). The Lagrange multiplier  $\zeta$  is a phase function,

$$\zeta(t) = \frac{\sum (\mathbf{p}/m) \cdot [\mathbf{F}(\mathbf{q}) + \mathcal{P}(\mathbf{q}, \mathbf{p})X]}{\sum (\mathbf{p} \cdot \mathbf{p})/m}, \quad (11)$$

which acts as a fluctuating thermostat variable. At equilibrium the long-time average,  $\langle \zeta \rangle$ , vanishes. If the phase-space dynamics is sufficiently mixing to make the system ergodic - as is usually the case even for two-particle systems due to the inherent Lyapunov instability - any time average is equivalent to an ensemble average with an equilibrium phase-space distribution function given by

$$f_0^{(G)} = C \exp\{-\beta\Phi(\mathbf{q})\} \delta(K(\mathbf{p}) - K_0), \quad (12)$$

where  $\beta = 1/kT$ . The temperature  $T$  is not explicitly contained in the equations of motion and enters the problem only through the initial conditions. Any numerical solution of (5) with (11) keeps the kinetic energy at that value it had at the beginning of the simulation. As usual, the normalization constant  $C$  ensures that the integral of the distribution function over all phase-space variables is unity. With respect to the momenta this so-called *isokinetic ensemble* is microcanonical.

The method of Gauss may also be used to fix the total internal energy  $H_0$ , not only its kinetic-energy contribution. The equations of motion remain the same as before, only the friction variable for the ensuing *isoenergetic ensemble* becomes

$$\zeta(t) = \frac{J(t)X}{\sum(\mathbf{p} \cdot \mathbf{p})/m}. \quad (13)$$

**Nosé - Hoover thermostat:** In some applications an algorithm is desired which generates a canonical ensemble in equilibrium. Such a new version of mechanics was invented by S. Nosé [20, 24] and put into a more practical form by W.G.Hoover [25, 1]. Assuming equations of motion with a thermostating force  $-\zeta\mathbf{p}$  as in (5), the thermostat variable  $\zeta$  is considered an additional independent variable, thus increasing the number of state variables by one. The time development of the phase-space density  $f(\mathbf{q}, \mathbf{p}, \zeta)$  in the extended  $(2dN + 1)$ -dimensional phase space is given by the continuity equation

$$\frac{\partial f}{\partial t} + \sum \frac{\partial}{\partial \mathbf{q}} \cdot (f\dot{\mathbf{q}}) + \sum \frac{\partial}{\partial \mathbf{p}} \cdot (f\dot{\mathbf{p}}) + \frac{\partial}{\partial \zeta} (f\dot{\zeta}) = 0, \quad (14)$$

which is a generalized version of the Liouville equation familiar from the statistical mechanics of Hamiltonian systems. At equilibrium ( $X = 0$ ), a steady-state solution ( $\partial f/\partial t = 0$ ) of (14) is obtained with the ansatz

$$f(\mathbf{q}, \mathbf{p}, \zeta) = C \exp(-\beta H_0)g(\zeta), \quad (15)$$

yielding a Gaussian for  $g(\zeta)$ . Thus,

$$f_0^{(N-H)}(\mathbf{q}, \mathbf{p}, \zeta) = C \exp(-\beta H_0(\mathbf{q}, \mathbf{p})) \exp(-\zeta^2 \tau^2/2) \quad (16)$$

is canonical. The parameter  $\tau$  determines the response time of the thermostat and should be chosen to be of the order of the duration of the fastest dynamical events in the system. The time variation of  $\zeta$  is obtained from the feedback equation

$$\dot{\zeta} = \frac{1}{\tau^2} \left( \sum \frac{\mathbf{p}^2}{mkT} - 1 \right). \quad (17)$$

(5) and (17) together constitute the Nosé-Hoover equations of motion, and the dimension of the phase space is increased by one:  $\Gamma = (\mathbf{q}, \mathbf{p}, \zeta)$ .

Both the Gaussian and Nosé-Hoover thermostats are capable of maintaining steady-state conditions for perturbed systems. At equilibrium the phase-space densities (12) and (15) are smooth functions of the phase variables. In nonequilibrium steady states, however, these functions become much more complicated strange attractors displaying a multifractal geometry. This complex topology lies at the heart of the difficulties of formulating a statistical theory for nonequilibrium processes and will be discussed in more detail in Section

5. In the following sections examples for algorithms involving mechanical and thermal perturbations will be given.

The Nosé-Hoover thermostat is not mixing enough to prevent regularity islands from surviving in the phase space of the one-dimensional harmonic oscillator [26]. Several workers have sought thermostats which will provide ergodic phase-space trajectories even for this simple case. All of the successful approaches involve introducing at least two thermostating variables rather than a single friction coefficient  $\zeta$ . In the more elaborate approaches thermostats can even be applied to rotational as well as translational degrees of freedom. Kusnezov and Bulgac have recently applied these ideas to a variety of classical and quantum systems [27, 28], including relatively small clusters of sodium atoms. They, with Bauer and others, have suggested and explored a wide variety of applications in nuclear physics, quantum path integrals, and quantum chromodynamics [27, 30]. It is clear that the evaluation and implementation of various thermostat types is in the early stages of vigorous growth.

## 2. Color Conductivity

As an example of a mechanical field we imagine a system of  $N$  particles of mass  $m$  in a three-dimensional box of volume  $V$ , which carry color charges  $c = \pm 1$ . The total system is assumed to be color neutral. The charges only interact with the external field  $\mathbf{X} = X\hat{x}$  where  $\hat{x}$  is a unit vector in  $x$ -direction. The perturbed Hamiltonian becomes

$$H = \sum \frac{\tilde{\mathbf{p}}^2}{2m} + \Phi - \sum cxX, \quad (18)$$

where  $\tilde{\mathbf{p}}$  is the total momentum of a particle canonical conjugate to  $\mathbf{q}$ . The color flux is associated with an averaged momentum in  $x$ -direction,  $\bar{p} = \sum c\tilde{p}_x/N$ , such that

$$\mathbf{p} = \tilde{\mathbf{p}} - \bar{p}\hat{x} \quad (19)$$

defines a peculiar momentum  $\mathbf{p}$ . We use a Gaussian thermostat to make the peculiar kinetic energy  $\sum \mathbf{p}^2/2m$  a constant of the motion. The equations of motion are

$$\dot{\mathbf{q}} = \frac{\tilde{\mathbf{p}}}{m} \quad (20)$$

$$\dot{\tilde{\mathbf{p}}} = \mathbf{F}(\mathbf{q}) + cX\hat{x} - \zeta\tilde{\mathbf{p}}, \quad (21)$$

where the thermostat variable becomes

$$\zeta = \frac{\sum(\mathbf{p}/m) \cdot (\mathbf{F} - (c/N)\sum c\mathbf{F})}{\sum(\mathbf{p} \cdot \mathbf{p})/m}. \quad (22)$$

As before, the adiabatic ( $\zeta = 0$ ) rate of change of the internal energy defines the dissipative flux  $J(t)$ ,

$$\dot{H}_0 = \sum c \frac{\tilde{p}_x}{m} X = N \frac{\bar{p}}{m} X = -JX. \quad (23)$$

Averaged over the initial equilibrium ensemble, the correlation function of this flux is given by the autocorrelation function of the  $x$ -component of the particle velocity,

$$\langle J(0)J(t) \rangle_0 = N \langle v_x(0)v_x(t) \rangle_0, \quad (24)$$

which together with the linear-response expression (2) and the Green - Kubo integral

$$D = \int_0^\infty dt \langle v_x(0)v_x(t) \rangle_0 \quad (25)$$

for the self-diffusion coefficient  $D$  yields the NEMD result

$$D = \lim_{X \rightarrow 0} \lim_{t \rightarrow \infty} \frac{\langle \bar{p} \rangle}{\beta X}. \quad (26)$$

This method has been shown to give results consistent with the equilibrium method based on the direct integration of (25) [22]. We have studied in detail the Lyapunov instability for this model [31] for up to 32 particles in three dimensions.

### 3. Homogeneous Shear Flow

A homogeneous method for the calculation of the shear viscosity provides a nice application of thermal driving. Let us consider planar Couette flow in  $x$ -direction, for which only a single component of the velocity-gradient tensor

$$\nabla \mathbf{u} = \begin{pmatrix} 0 & 0 \\ \dot{\epsilon} & 0 \end{pmatrix}; (\nabla u)_{ij} \equiv \partial u_j / \partial q_i \quad (27)$$

is different from zero and where the shear rate  $\dot{\epsilon}$  assumes the role of the fictitious field. The so-called SLLOD-equations of motion

$$\begin{aligned} \dot{x} &= (p_x/m) + y\dot{\epsilon} \\ \dot{y} &= (p_y/m) \\ \dot{p}_x &= F_x - p_y\dot{\epsilon} - \zeta p_x \\ \dot{p}_y &= F_y - \zeta p_y \end{aligned} \quad (28)$$

cannot be derived from a Hamiltonian. However, the Doll's tensor equations of motion, which give exactly the same correct linear viscosity coefficient, do follow from a Hamiltonian [32, 33]. In the limit of vanishing  $\dot{\epsilon}$  equations (28) are consistent with the linear-response result. This may be seen most easily by recalling the Green-Kubo integral for the shear viscosity  $\eta$ ,

$$\eta = \beta V \int_0^\infty dt \langle P_{xy}(0)P_{xy}(t) \rangle_0, \quad (29)$$

where  $P_{xy}$  is the  $xy$ -component of the microscopic pressure tensor

$$\mathbf{P} = \frac{1}{V} \left( \sum_i \frac{\mathbf{p}_i \mathbf{p}_i}{m} + \sum_{i < j} \mathbf{F}_{ij} \mathbf{q}_{ij} \right). \quad (30)$$

$\mathbf{F}_{ij}$  is the force on particle  $i$  due to particle  $j$ . It follows from (1) that the dissipative flux  $J(t) = VP_{xy}$ . The same result is obtained from the adiabatic time dependence of the internal energy according to (9), if the equations of motion (28) are inserted. This proves our assertion. The NEMD-expression for the viscosity is therefore

$$\eta = \lim_{t \rightarrow \infty} \lim_{\dot{\epsilon} \rightarrow 0} - \frac{\langle P_{xy}(t) \rangle}{\dot{\epsilon}}. \quad (31)$$

It is obvious from (28) that the momenta  $\mathbf{p}$  are peculiar with respect to the hydrodynamic streaming velocity  $\mathbf{u} = u(y)\hat{\mathbf{x}}$  in  $x$ -direction. Although it might appear that this restricts the applicability of (28) to low-Reynolds number laminar flow, it is known that the SLLOD equations are accurate even arbitrarily far from equilibrium. Only the notion of a kinetic temperature has to be reinterpreted for turbulent flow. In fact, this is the only NEMD-algorithm known to be correct in this sense if the thermostat is removed.

To obtain a homogeneous method the motion equations (28) have to be used in combination with suitable periodic boundary conditions consistent with the shear. Such conditions were formulated by Lees and Edwards [34]. If the basic simulation box is a square with length  $L$  such that the lower left corner coincides with the origin, the Lees - Edwards boundary conditions can be compactly written as

$$\begin{aligned} x_{new} &= (x_{old} \pm \dot{\epsilon}Lt) \bmod (L) \\ y_{new} &= y_{old} \bmod (L) \\ \dot{x}_{new} &= \dot{x}_{old} \pm \dot{\epsilon}L \\ \dot{y}_{new} &= \dot{y}_{old}, \end{aligned} \tag{32}$$

where  $t$  is the time elapsed from the beginning of the shear, and  $+/-$  refers to a particle crossing the lower/upper boundary with negative/positive  $\dot{y}$ . Similar considerations also apply to the calculation of the minimum-image particle positions and velocities.

So far we have not mentioned the thermostat terms  $-\zeta\mathbf{p}$ . Either Gaussian or Nosé-Hoover thermostats may be employed. Since in the simple version outlined above both methods use a kinetic-temperature definition (14) based on peculiar momenta  $\mathbf{p}$  they are "biased" with respect to the linear velocity profile required by (27). These "profile-biased thermostats" lead to a "string phase" at intermediate and higher shear rates in which the particles align themselves like the pearls of a necklace stretched in the direction of the shear [17]. This phenomenon is accompanied by a significant reduction of the viscosity. Any deviation from the linear velocity profile caused by a breakup of such a string is interpreted by the thermostat as additional heat which it tries to remove stabilizing the strings in turn. To remove such interference local thermostats - "profile unbiased thermostats" - have been introduced by partitioning the simulation box and calculating local streaming velocities by averaging over all particles within the different partitions. These precautions do not remove totally shear-induced ordering at large shear rates. Coexisting ordered and amorphous particle configurations have been found, and the instantaneous velocity profile may deviate considerably from linearity. There is still no unanimous agreement about the physical significance of these results. Since a test in real liquids would require such high shear rates totally inaccessible in the laboratory, a partial verification of these results has so far been found only in experiments with colloidal suspensions [38, 39].

The last remarks apply only to simulations with very large shear rates. For the determination of shear viscosities based on (31), the SLLOD and the Doll's-Tensor method are very efficient and successful. Good agreement with equilibrium results and laboratory experiments have been achieved.

A modification of the previous method has been used for the simulation of bulk viscosity [33]. Also homogeneous algorithms for the evaluation of heat conductivity have been formulated by Evans [35] and Gillan [36]. Both methods lead to the same results and are in agreement with linear response theory [37].

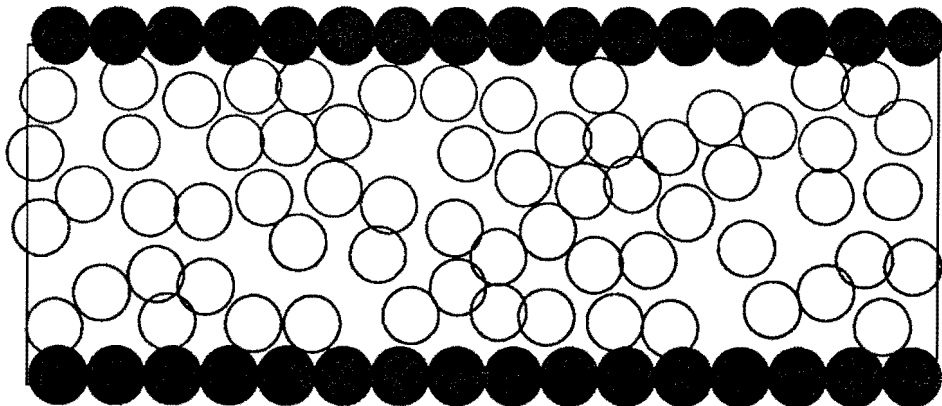


Figure 1: Snapshot of a shear-flow simulation with WCA potential model (B) of section 4. The upper wall moves to the right with velocity  $\dot{\epsilon}l/2$ , the lower accordingly to the left. The shear rate  $\dot{\epsilon} = 2$ , and the vertical separation of the interaction-site centers of the opposite walls  $l = 6$ .  $N = 64$  Hamiltonian particles at a density  $n = N\sigma^2/V = 0.8$  are sheared. The interaction sites on one wall are separated by unity. Lennard-Jones reduced units are used.

### Boundary-driven Shear Flow

Actually there is no need at all to introduce the shear rate-containing terms in the equations of motion (28) to generate Couette flow. It suffices to implement only the Lees-Edwards boundary conditions (32) to establish shear flow with a linear velocity profile after some transients have died out. Any particle entering the simulation box from above/below carries on the average a positive/negative momentum component in  $x$ -direction which helps to build up the shear.

An even simpler method consists in renouncing periodic boundaries perpendicular to the shear altogether and to study particle flow between two moving thermostatted walls. Historically this was the first NEMD method to be studied. As compared to the homogeneous algorithm described in the previous section it suffers from several deficiencies: Firstly, there is severe local order of the fluid particles in the neighborhood of the reflecting walls [11]. Therefore huge particle numbers are required if bulk values for  $\eta$  are desired. This local order can be substantially reduced by using flexible fluid walls" [14]. Secondly, for larger shear rates the fluid may easily decouple from one of the walls leading to shear-induced formation of amorphous solids. Thirdly, total momentum is not conserved. However, this method offers the big advantage that the number of thermostatted degrees of freedom can be made relatively small such that the dynamics of almost all particles is determined by unthermostatted Hamilton's equations. For this reason we have carried out extensive simulations with such a system [40, 41, 42] which we describe next. The theoretical implications of these results are far reaching and are discussed in Section 5.

We consider a two-dimensional fluid as shown in Fig.1, bounded in the  $y$ -direction by two moving walls and separated by  $l$ . Each wall consists of rigidly connected interaction

centers  $\sigma$  apart. The  $N$  fluid particles interact with each other and with the boundary interaction sites, and their dynamics is governed by Hamilton's equations of motion:

$$\begin{aligned}\dot{\mathbf{q}}_f &= \mathbf{p}_f/m \\ \dot{\mathbf{p}}_f &= -\nabla_f(\Phi_f + \Phi_{int}).\end{aligned}\quad (33)$$

$\Phi_f$  is the potential energy between the Hamiltonian bulk particles taken to be pairwise additive, and  $\Phi_{int}$  is the interaction energy between the bulk particles and the boundary. In the horizontal  $x$ -direction periodic boundary conditions apply. The boundary interaction sites move in a coherent fashion according to two types of motion:

- a constant driving velocity  $+/- \dot{\epsilon}l/2$  of the upper/lower boundary in  $x$ -direction,
- a Nosé-Hoover thermostat acting isotropically in  $x$ - and  $y$ -direction.

The respective equations of motion are given by

$$\begin{aligned}\dot{\mathbf{x}}_b &= \mathbf{p}_b/m \pm \dot{\epsilon}(l/2)\hat{\mathbf{x}} \\ \dot{\mathbf{p}}_b &= -\nabla_b\Phi_{int} - \zeta\mathbf{p}_b \\ \dot{\zeta} &= [\mathbf{p}_b^2/(2mkT) - 1]/\tau^2.\end{aligned}\quad (34)$$

The mass of each bulk particle is  $m$  as is also the combined mass of the coherently joined interaction sites. Two models for the potential energies were studied:

**Model A:**  $\Phi_f$  and  $\Phi_{int}$  are sums over a specially smooth repulsive pair potential

$$\phi(r) = \begin{cases} \epsilon[1 - (r/\sigma)^2]^4 & , r < \sigma \\ 0 & , r \geq \sigma \end{cases}\quad (35)$$

To avoid the escape of bulk particles through the boundaries an additional short-ranged purely repulsive Lennard-Jones interaction  $4\epsilon[(\hat{\sigma}/s)^{12} - (\hat{\sigma}/s)^6] + \hat{\epsilon}$  for  $s \equiv |y_b - y_f| < 2^{1/6}\hat{\sigma}$  is included in  $\Phi_{int}$ . This added repulsion depends only on the normal separation of a bulk particle from the boundary. Alternatively a hard elastic wall can be introduced. Reduced units are used for which  $\epsilon = 100$ ,  $\sigma = 1$ ,  $\hat{\sigma} = 1/10$  and  $k = 1$ . Details of the results for this model are given in Refs. [40] and [41].

**Model B:**  $\Phi_f$  and  $\Phi_{int}$  are made up of sums of repulsive Lennard Jones potentials

$$\phi(r) = \begin{cases} 4\epsilon[(\sigma/r)^{12} - (\sigma/r)^6] + \epsilon & , r < 2^{1/6}\sigma \\ 0 & , r \geq 2^{1/6}\sigma \end{cases}\quad (36)$$

Reduced units are used, for which  $\epsilon$ ,  $\sigma$ ,  $m$ , and  $k$  are unity. Details of simulation results for this model will be given elsewhere [42].

The phase space of this shear flow calculation is  $(4N + 6)$ -dimensional,  $4N$  dimensions are being accounted for by the Hamiltonian bulk particles. The 6 dimensions include the friction coefficient  $\zeta$  and an additional variable  $\epsilon$  due to the relative shear displacement of the boundary interaction sites, for which we may take the time or the shear. The shear variable  $\epsilon$  was overlooked in one of our earlier papers [40]. Since momentum is not conserved for this model the whole simulation box may float around, and the four variables  $\{x_b, y_b, p_{b,x}, p_{b,y}\}$ , along with  $\epsilon$ , are required to fix unambiguously the location of the boundary. Thus, the overwhelming contribution to the phase-space dimension comes from the bulk particles

obeying Hamilton's equations (33), and only a very small number, namely 6, is due to the non-Hamiltonian thermostatted boundary.

## 5. Lyapunov Instability and the Second Law

The Gibbs entropy of a nonequilibrium system is defined by

$$S(t) = -k \int d^L \Gamma f(\Gamma, t) \ln f(\Gamma, t), \quad (37)$$

where  $L$  is the phase-space dimension and  $\Gamma = \{\mathbf{q}, \mathbf{p}, \zeta\}$  is the state vector. For the rate of change of  $S$  we find

$$\dot{S}/k = \int d^L \Gamma f(\Gamma, t) \left( \frac{\partial}{\partial \Gamma} \cdot \dot{\Gamma} \right) = \left\langle \frac{\partial}{\partial \Gamma} \cdot \dot{\Gamma} \right\rangle, \quad (38)$$

where the continuity equation (25) and integration by parts has been used at one stage [43]. If the last expression is evaluated for a particular model such as the thermostatted shear problems discussed before by inserting the respective equations of motion one finds

$$\dot{S}/k = - \sum_{TDOF} \langle \zeta \rangle. \quad (39)$$

The sum in this expression is over the thermostatted degrees of freedom, contributing a factor of 2 for the boundary-driven shear equations (33) and (34). In nonequilibrium steady states the thermostat constantly removes heat from the system to keep the temperature constant.  $\langle \zeta \rangle$  is therefore always *positive*. From (39) we conclude that the Gibbs entropy diverges to  $-\infty$  for  $t \rightarrow \infty$ . From this we conclude that the phase-space density  $f(\Gamma, t)$  develops singularities and does not stay smooth and well behaved for nonequilibrium steady states thermostatted by one of the thermostats described above. The phase-space distribution collapses onto an attracting subset of the phase space with a fractal dimension less than the dimension  $L$ .

This collapse onto a strange attractor is easily visualized for low-dimensional systems with phase-space dimension  $L = 3$ , by looking at a two-dimensional Poincarè section. In earlier studies we have demonstrated this

(a) for a *one-dimensional color-conductivity model* of a single particle in a sinusoidal potential and subjected to a constant external field [44, 45]. The particle is thermostatted by a Nosé-Hoover thermostat.

(b) for the *Galton-board* problem of a point particle falling - under the influence of an accelerating field - through a triangular-lattice array of hexagonally arranged scatterers [46]. The absolute value of the falling particle's momentum was kept a constant by invoking a Gaussian thermostating procedure.

Both examples have a three-dimensional phase space and their Poincarè sections are fractal. Analogous problems such as periodic two-body hard-disk shear flow or two-body shear flow using the WCA potential [47] lead to similar results.

To establish a more quantitative basis for the discussion we have evaluated for the two aforementioned models the generalized Renyi dimensions  $D_q$  defined by

$$D_q = \frac{1}{1-q} \lim_{\epsilon \rightarrow 0} \frac{\ln \sum_i p_i^q(\epsilon)}{\ln(1/\epsilon)}. \quad (40)$$

Here we imagine a partition of the phase space with boxes of size  $\epsilon$ .  $p_i(\epsilon)$  is the natural measure (probability) of the attractor attributed to box  $i$ ,  $p_i = \int_i d\mu$ .  $D_0$  is called the "capacity" and is a simplified version of the well-known Hausdorff dimension [48]. It is the dimension of the support of the measure.  $D_1$  is the "information dimension" and reflects the dimension of the natural measure  $\mu$ . For all applications in this paper this is the most important parameter. From a practical point of view it is more convenient to evaluate the multifractal spectrum of singularities [49, 50, 51]  $f(\alpha)$ , where  $\alpha$  is the singularity strength, for which a canonical algorithm has been given by Chhabra and Jensen [52]. The Renyi dimensions can then be obtained from  $f(\alpha)$  by a negative Legendre transformation,

$$\tau(q) \equiv (q-1)D_q = q\alpha(q) - f(\alpha(q)), \quad (41)$$

and

$$\alpha(q) = \frac{d\tau(q)}{dq}. \quad (42)$$

The results of these calculations may be summarized as follows: Firstly, for all models a well defined singularity spectrum  $f(\alpha)$  is obtained, and the generalized dimensions are not equal. This shows that the phase-space attractors are actually *multifractals*, which may be imagined as an interwoven fractal set of fractals. Secondly, for the conductivity model (a) the capacity  $D_0 = 2.63$  is significantly smaller than the phase-space dimension, and the information dimension with  $D_1 = 2.47$  is even smaller, as required also by theory. For the Galton-board model (b) we find  $D_0 \approx 3$  which is equal - to within the statistical uncertainty - to the phase-space dimension. The information dimension is significantly smaller again. It looks as if the whole phase space acts as a support for the strange attractor. We believe that this is the generic situation for two- and three-dimensional many-body systems in nonequilibrium steady states. The natural probability distribution, however, is always confined to a subset with reduced dimensionality  $D_1$  and consequently has a vanishing phase-space volume.

Unfortunately, the methods of dimensional analysis just described are not really applicable to many-body systems. If we subdivide each phase-space direction into 10 bins, and if we imagine a 100-particle system in two dimensions with a phase-space dimension  $L = 400$  - certainly not exaggerated assumptions by any standards - a box-counting algorithm for the evaluation of  $f(\alpha)$  or  $D_q$  would require  $10^{400}$  boxes. By far the whole universe would not suffice to store the required information. However, there is a way to bypass that hurdle by computing the Lyapunov characteristic exponents instead, from which  $D_1$  may be obtained using an idea due to Kaplan and Yorke [53].

Any chaotic system is characterized by its sensitivity due to small perturbations of the initial conditions. A nearby trajectory in phase space will on the average get separated exponentially with time from the reference trajectory. Let us imagine perturbed trajectories with initial phases on a differentially small hypersphere centered on the reference trajectory. Due to the phase flux this sphere will quickly develop into a hyperellipsoid with comoving principle axes expanding or contracting exponentially. The associated time-averaged rate

constants constitute the set of Lyapunov characteristic exponents  $\lambda_l, l = 1, \dots, L$ , also called the Lyapunov spectrum. For chaotic motion at least one of the exponents has to be positive. A number of algorithms for their evaluation have been reported. The computation of one of the exponents requires the solution of  $L$  linear first-order differential equations obtained from linearizing the original nonlinear equations of motion. The computation of the whole Lyapunov spectrum therefore requires the simultaneous solution of  $L(L + 1)$  coupled first-order differential equations, leading to 160400 equations for the example given above. This number constitutes a practical upper limit for present-day computers. Massively-parallel computation will certainly permit a substantial increase in the number of system particles in the near future [54].

The Lyapunov exponents are conventionally arranged from largest to smallest,  $\lambda_1 \geq \lambda_2 \geq \dots \geq \lambda_L$ . Their total sum is equal to the averaged logarithmic rate of phase-volume expansion and also equal to  $\sum_{th} \dot{Q}/kT$ , where  $Q$  is the outgoing heat extracted by the frictional forces characterized by a kinetic temperature  $T$ . The sum is over all thermostats, if more than one are used. Because of (38) and (39) this leads to the important chain of equalities

$$\sum_{th} \dot{Q}/kT = - \left\langle \frac{\partial}{\partial \Gamma} \cdot \dot{\Gamma} \right\rangle = - \sum_{l=1}^L \lambda = \sum_{TDOF} \langle \zeta \rangle > 0. \quad (43)$$

This means that for a Hamiltonian system or for a thermostatted system in equilibrium the sum over all Lyapunov exponents vanishes. For such systems the spectra exhibit also a pronounced symmetry: for each positive exponent there is another negative exponent with equal absolute magnitude, forming a so-called Smale pair [31]. For Hamiltonian systems the origin of this pairing lies in the symplectic nature of the equations of motion, which means that the phase flow - viewed as a canonical transformation of the phase space onto itself - leaves the differential two-form  $\sum_{i=1}^{L/2} dp_i \wedge dq_i$  invariant [55]. This symmetry also persists for thermostatted equilibrium systems as has been shown explicitly for Gaussian thermostats by Evans and coworkers [56]. For driven systems in nonequilibrium steady states the sum of all Lyapunov exponents is negative, as follows from (43). For *homogeneously driven* systems, that is for thermostats affecting every particle momentum with a single  $\zeta$ , the symmetry for the Smale pairs  $\lambda_i, \lambda_{L-i+1}$  takes the simple form [56]

$$\lambda_i + \lambda_{L-i+1} = -\langle \zeta \rangle. \quad (44)$$

The whole Lyapunov spectrum appears to be shifted to more negative values [31]. This very striking pairing symmetry (44), however, does not hold for *inhomogeneous* systems such as the boundary-driven planar Couette-flow model (A) introduced in Section 4.

In Fig.2 we show a full spectrum for such a system containing  $N = 96$  bulk particles at a particle density  $n = N\sigma^2/V = 0.8$ . The thermostat response time  $\tau = 0.02$ . The phase-space dimension for this problem is  $L = 4 \times 96 + 6 = 390$ . 389 exponents are shown in the figure. The extra exponent due to the boundary periodicity - as discussed in the previous section - vanishes because of the regularity of this motion and need not be calculated explicitly. The exponents are arranged such that pairs of exponents are given the same index on the abscissa, the largest exponent pairing with the smallest, the largest but one with the smallest but one, and so forth. The strong asymmetry of the spectrum is striking. Only 6 of the independent variables of the problem are associated with the thermostatted boundary, and they are mainly responsible for the pronounced asymmetry. In the insert,

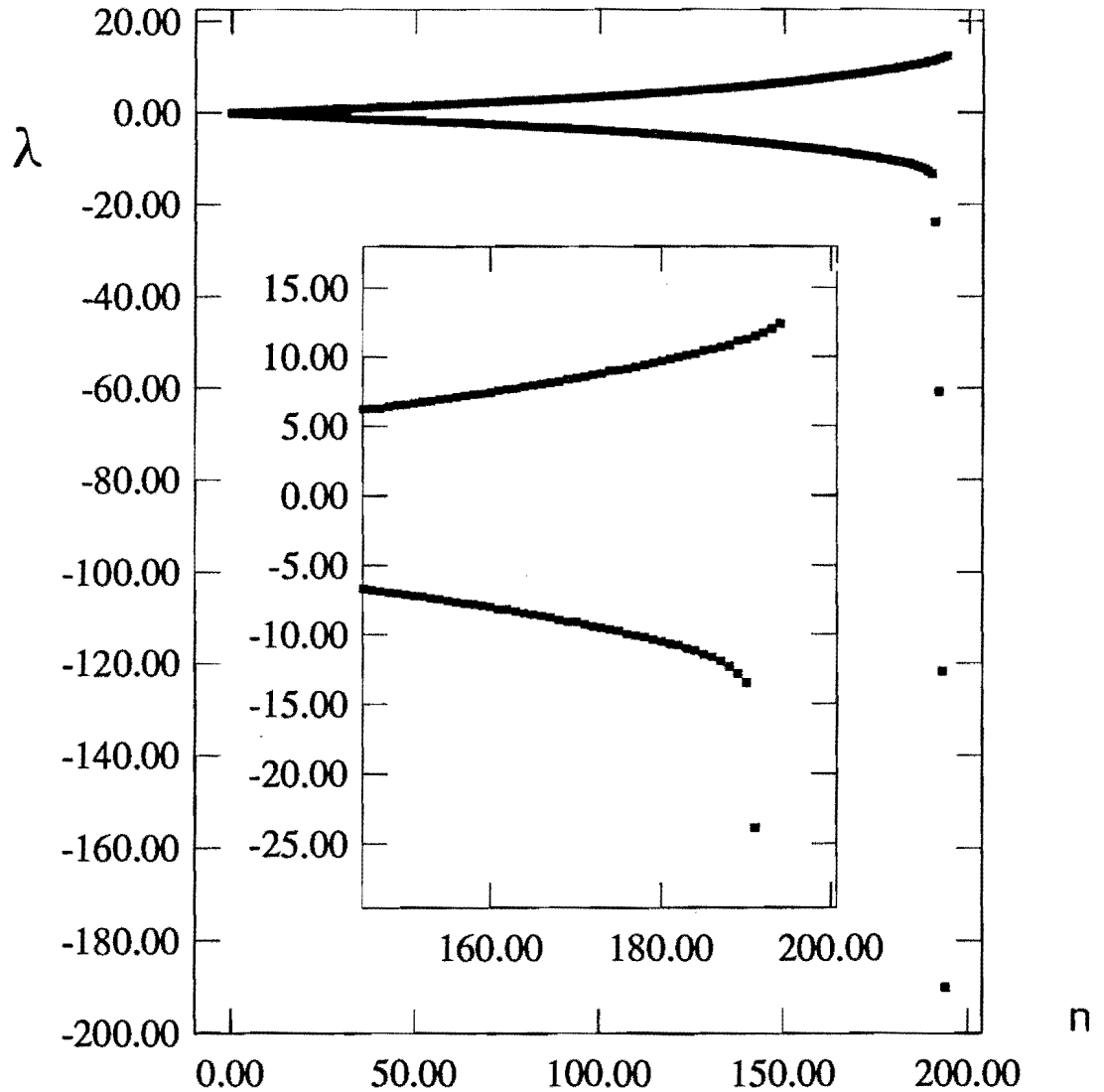


Figure 2: Lyapunov spectrum obtained with the inhomogeneously-driven planar Couette-flow model (A) described in Section 4. Small-pairs of exponents are given the same index  $n$  plotted on the abscissa. Details of the simulation run involving 96 bulk particles and 48 coherently moving interaction sites - 24 on each boundary - are given in the main text. The insert is a magnification of the upper right corner of the spectrum.

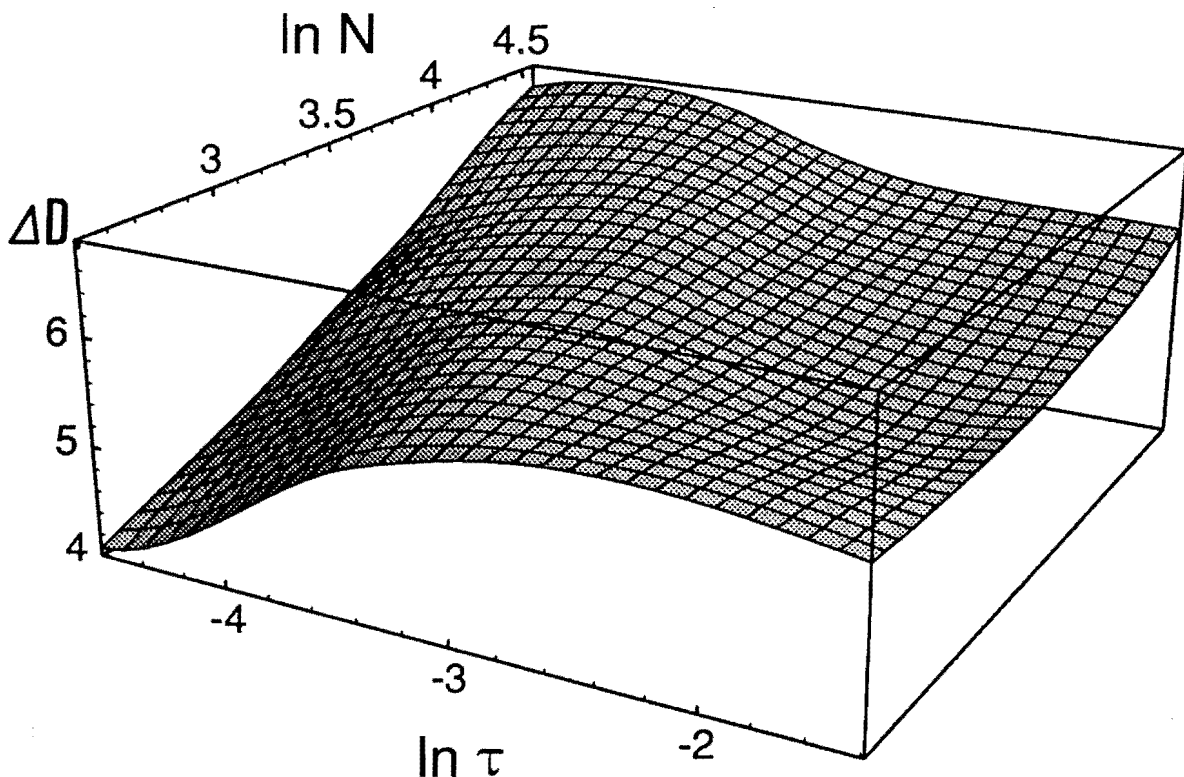


Figure 3: The surface  $\Delta D$  of the dimensionality reduction for the boundary-driven shear model (A) of Section 4 as a function of the thermostat response time  $\tau$  and the bulk-particle number  $N$ . The surface was constructed from 49 simulation points with cubic-spline interpolation.

which depicts the enlarged upper right corner, the overall shift to more negative values is clearly visible - similar to the homogeneously thermostatted case.

Once the full spectrum of Lyapunov exponents are known, the information dimension of the subspace effectively visited by the trajectory can be calculated. Kaplan and Yorke pointed out that any volume on that subspace should be an invariant of the phase flux which implies that the sum of all positive exponents has to be cancelled exactly by a certain number of negative exponents [53]. If the cumulative sum  $\mu(J) \equiv \sum_{i=1}^J \lambda_i$  (with  $\lambda_i \geq \lambda_{i+1}$ ) changes sign between  $J$  and  $J+1$ , the fractal dimension of the attractor is then obtained by linear interpolation:

$$D_1 = J + \frac{\mu(J)}{|\lambda_{J+1}|}. \quad (45)$$

For the example given in Fig.2 with  $L = 4 \times 96 + 6 = 390$  one obtains  $D_1 = 383.21$  in the complete phase space with  $\varepsilon$  included. We therefore find a reduction in dimensionality  $\Delta D \equiv L - D_1 = 6.79$ .

We have evaluated  $\Delta D$  for both boundary-driven shear-flow models introduced in Section 4, where the number of bulk particles,  $N$ , varied between 16 and 96. The bulk-particle density was kept constant,  $n = N\sigma^2/V = 0.8$ , and the wall separation with  $l = 6$  and the shear rate  $\dot{\varepsilon} = 2$  were the same for all runs, The length of the simulation box in the

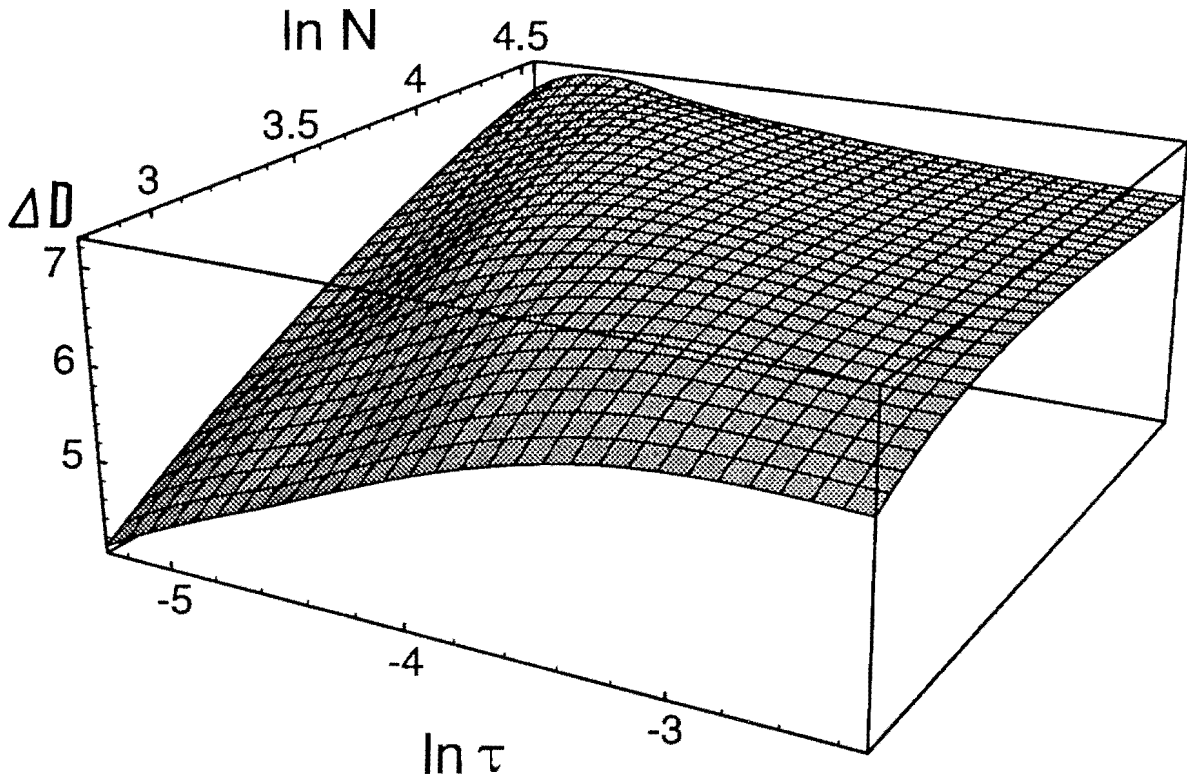


Figure 4: The surface  $\Delta D$  of the dimensionality reduction for the boundary-driven shear model (B) of Section 4 as a function of the thermostat response time  $\tau$  and the bulk-particle number  $N$ . The surface was constructed from 42 simulation points with cubic-spline interpolation.

shearing direction varied between 4 and 24, and the number of interaction sites for the coherent “wall particle” between 8 and 48. In Fig.3 we display the surface  $\Delta D(\ln \tau, \ln N)$  for model (A), and in Fig.4 for model (B). As defined in (34),  $\tau$  is the response time of the Nosé-Hoover thermostat acting solely on the boundary. The kinetic temperature is unity for all runs. Figures 3 and 4 show that for fixed  $N$  one finds a maximum for the dimensionality reduction for a certain  $\tau$  which shifts to smaller values as the number of bulk particles is increased. Evidently there is a resonance which enhances boundary coupling and mixing in phase space and increases the dimensionality reduction whenever the response time of the thermostat is about equal to the collision time of the bulk. Viewed as a function of  $N$ , the maximum dimensionality reduction seems to increase roughly logarithmically with the number of bulk particles [42].

The dimensionality reduction for the WCA - potential model (B) is consistently larger than that for model (A). Such a result is to be expected since the repulsive potential of model (B) is much steeper, which enhances the Lyapunov instability.

The appearance of a strange attractor for the phase-space distribution readily explains why such thermostatted nonequilibrium steady-state systems always correspond to irreversible computer solutions associated with positive transport coefficients in spite of the fact that the equations of motion are time reversible [57, 45] Trajectories capable of violating the Second Law of thermodynamics would have to lie on the strange repeller, an unstable

set of states obtained from the strange attractor by the time-reversal transformation  $\vartheta$  of Section 1. Since the dimension  $D_1$  of both strange sets is smaller than the phase-space dimension  $L$ , their phase volume has to vanish, and Second Law-violating states occur only with measure zero. Due to the instability of the repeller, trajectories near the repeller are quickly diverted and eventually end up on the attractor again.

## 6. Fractal Phase-space Distributions

In the previous section we have shown that the key property of a thermostatted nonequilibrium system satisfying appropriate constraints is the fractal, even multifractal, structure of its phase-space density  $f(\Gamma, t)$ . It provides a geometrical interpretation of their macroscopic irreversible behavior in spite of the microscopic reversibility of the underlying equations of motion by establishing a link with the chaotic properties associated with the Lyapunov instability and quantified by the spectrum of Lyapunov exponents. This interesting result - if it is proven to be valid also for macroscopic transport studied experimentally in the laboratory and not just for computer ensembles with a few constraints - enormously complicates the formulation of a theory of nonequilibrium processes and explains why no satisfying theory presently exists:  $f(\Gamma, t)$  cannot be treated as a smooth and differentiable function any more. The significance of these results has been questioned, by Lebowitz and Link [58, 41]. They refer to rigorous results for a heat-conductivity system thermostatted by Gaussian thermostats for which the phase-space distribution is non-fractal and analytic [59, 60]. Obviously stochastic boundary conditions smear out the intricate fractal structure in phase space. But they are not time reversible and therefore should not be used for a deterministic description of transport.

It is interesting to note that a distribution function of an inhomogeneously thermostatted system can still remain fractal, even if it is projected down onto a subspace by integrating over all independent variables directly associated with the thermostat, which are  $\{x_b, y_b, p_{b,x}, p_{b,y}, \zeta, \varepsilon\}$  for the boundary-driven shear-flow problems of Section 4. This may be seen by inspection of Figs. 3 and 4. For large-enough systems the dimensionality reduction  $\Delta D$  can exceed six, the dimension contributed by these extra variables. Even projecting down onto the subspace of the boundary particles leaves the reduced phase-space distribution a fractal.

Fractal structures in phase space might well be expected also from another point of view. Jaynes' [61] and Zubarev's [62] maximum-entropy approach to nonequilibrium ensembles maximizes the uncertainty in the distribution of phase-space states satisfying appropriate constraints. Consider for simplicity a three-dimensional fluid undergoing heat flow. Among the microcanonical  $(N, V, E)$  states making up a  $L$ -dimensional phase-space region, with specified composition, volume, and energy, those states having a particular heat flux vector  $\mathbf{Q}$  would occupy a  $L - 3$  dimensional subspace, with zero hypervolume relative to the equilibrium distribution. If we further restricted our maximum-entropy ensemble to include only those states with  $d\mathbf{Q}/dt$  equal to zero, the dimensionality would be further reduced. Further constraints on higher derivatives would further reduce the available phase-space states [63].

Interestingly, even in a non-thermostatted Hamiltonian system subjected to a periodic perturbation fractal structures may be found. It seems that all initial states violating the Second Law during one cycle of the perturbation are located on a fractal subspace with

vanishing phase volume. Precisely this behavior has been found in the thermodynamic limit of an exactly solvable model, an ensemble of noninteracting linear harmonic oscillators, for which the stiffness of the springs varies periodically in time [64]. All initial states which lead to a lower energy of the system after completion of one cycle of the perturbation - which would be called *active* in the sense of Pusz and Woronowicz [65, 66] - are located on a Cantor space-like structure with measure zero. The complementary so-called *passive* states, leading to an increase of the system's energy in accord with the Second Law, occupy almost the whole phase space with measure one in the thermodynamic limit.

In general nonequilibrium steady-state systems occupy *fractal* attractors with non-integral dimensionality, so that Gibbs' definition of entropy (relative to equilibrium) as the logarithm of phase hypervolume (relative to equilibrium) diverges. It seems likely that ongoing advances in parallel computing will make it possible to characterize this dimensionality loss in detail.

### Acknowledgments

We thank Joel Lebowitz and Gregory Eyink for their thoughtful comments concerning properties of phase-space distributions, and Gerhard Krexner for his help with the graphics program producing Figures 3 and 4. The considerable computational resources were provided by the Computer Center of the University of Vienna, operating within the framework of IBM's European Academic Supercomputer Initiative (EASI), and the Austrian Fonds zur Förderung der wissenschaftlichen Forschung, grant P8003, and are most gratefully acknowledged. Work at the Lawrence Livermore National Laboratory, performed under the auspices of the Department of Energy, was supported by Contract W-7405-Eng-48.

### References

- [1] W. G. Hoover, *Computational Statistical Mechanics*, Studies in Modern Thermodynamics 11 (Elsevier, Amsterdam, 1991).
- [2] G. Ciccotti and W. G. Hoover (eds.), *Molecular-Dynamics Simulation of Statistical - Mechanical Systems*, Course XCVII of Proc. Int. School of Physics Enrico Fermi, Varenna, (North-Holland, Amsterdam, 1986).
- [3] M. P. Allen and D. J. Tildesley, *Computer Simulations of Liquids* (Clarendon Press, Oxford, 1987).
- [4] M. S. Green, J. Chem. Phys. **20**, 1281 (1952); **22**, 398 (1954).
- [5] R. Kubo, J. Phys. Soc. (Jpn.) **12**, 570 (1957).
- [6] R. Zwanzig, Ann. Rev. Phys. Chem. **16**, 67 (1965).
- [7] B. J. Alder and T. E. Wainwright, Phys. Rev. A **1**, 18 (1970).
- [8] B. J. Alder and E. E. Alley, in *Perspectives in Statistical Physics*, edited by H. J. Raveche (North-Holland, Amsterdam, 1981), p. 3.
- [9] W. G. Hoover and W. T. Ashurst, Adv. Theor. Chemistry **1**, 1, 1975.

- [10] D. J. Evans and G. P. Morriss, *Statistical Mechanics of Nonequilibrium Liquids* (Academic Press, London, 1990).
- [11] S. Y. Liem, D. Brown and J. H. R. Clarke, *Phys. Rev. A* **45**, 3706 (1992).
- [12] B. Holian and D. J. Evans, *J. Chem. Phys.* **83**, 3560 (1985).
- [13] D. J. Evans and G. P. Morriss, *Molec. Phys.* **64**, 521 (1988).
- [14] W. T. Ashurst, Ph. D. Thesis, University of California at Davis, 1974.
- [15] B. L. Holian and D. J. Evans, *J. Chem Phys.*, **78**, 5147 (1983).
- [16] G. Ciccotti, G. Jacucci and I. R. McDonald, *Phys. Rev A* **13**, 426 (1976); *J. Stat. Phys.* **21**, 1 (1979).
- [17] W. Loose and G. Ciccotti, *Phys. Rev. A* **45**, 3859 (1992).
- [18] W. Loose and S. Hess, *Physica A* **174**, 47 (1991).
- [19] A. Baranyai and D. J. Evans, *Molec. Phys.* **74**, 353 (1991).
- [20] S. Nosé, *Molec. Phys.* **52**, 255 (1984).  
] D. J. Evans, *J. Chem. Phys.* **78**, 3297 (1983).
- [22] D. J. Evans, W. G. Hoover, B. H. Failor, B. Moran A. J. C. Ladd, *Phys. Rev. A* **28**, 1016 (1983).
- [23] A. Sommerfeld, *Vorlesungen über Theoretische Physik, Band 1: Mechanik*, Akademische Verlagsgesellschaft, Leipzig, 1962.
- [24] S. Nosé, *J. Chem. Phys.* **81**, 511 (1984).
- [25] W. G. Hoover, *Phys. Rev. A* **31**, 1695 (1985).
- [26] H. A. Posch, W. G. Hoover and F. J. Vesely, *Phys. Rev. A* **33**, 4253 (1986).
- [27] D. Kusnezov, A. Bulgac and W. Bauer, *Annals of Physics* **204**, 155 (1990); **214**, 180 (1992).
- [28] R. G. Winkler, *Phys. Rev. A* **45**, 2250 (1992).
- [29] G. J. Martyna, M. L. Klein and M. Tuckerman, "Nosé-Hoover Chains: the Canonical Ensemble via Continuous Dynamics" (Preprint, 1992).
- [30] A. Bulgac and D. Kusnezov, *Phys. Rev B* **45**, 1988 (1992).
- [31] H. A. Posch and W. G. Hoover, *Phys. Rev. A* **38**, 473 (1988).
- [32] W. G. Hoover, *Lecture Notes in Physics* **132**, *Systems far from equilibrium*, edited by: J. Ehlers et alii (Springer-Verlag, Berlin, 1980) p. 373.
- [33] W. G. Hoover, D. J. Evans, R. B. Hickman, A. J. C. Ladd, W. T. Ashurst and B. Moran, *Phys. Rev. A* **22**, 1690 (1980).

- [34] A. W. Lees and S. F. Edwards, *J. Phys. C* **5**, 1921 (1972).
- [35] D. J. Evans, *Phys. Lett. A* **91**, 457 (1982); *Phys. Rev. A* **34**, 1449 (1986).
- [36] M. J. Gillan and M. Dixon, *J. Phys. C* **16**, 869 (1983).
- [37] D. MacGowan D. J. Evans, *Phys. Lett. A* **117**, 414 (1986).
- [38] W. Loose and S. Hess, *Rheologica Acta* **28**, 91 (1989).
- [39] B. J. Ackerson, *Physica A* **174** 15 (1991).
- [40] H. A. Posch and W. G. Hoover, *Phys. Rev. A* **39**, 2175 (1989).
- [41] W. G. Hoover, H. A. Posch and C. G. Hoover, *Chaos* **2**, 2 (1992).
- [42] H. A. Posch and W. G. Hoover, in preparation.
- [43] B. L. Holian, *Phys. Rev. A* **34**, 4238 (1986).
- [44] W. G. Hoover, H. A. Posch, B. L. Holian, M. J. Gillan, M. Mareschal and C. Massobrio, *Molec. Simulation* **1**, 79 (1997).
- [45] H. A. Posch, W. G. Hoover and B. L. Holian, *Ber. Bunsenges. Phys. Chem.* **94**, 250 (1990).
- [46] W. G. Hoover and B. Moran, *Phys. Rev. A* **40**, 5319 (1989).
- [47] G. P. Morriss, *Phys. Lett A* **143**, 307 (1989); *Phys. Rev. A* **39** 4811 (1989).
- [48] J. D. Farmer, E. Ott and J. A. Yorke, *Physica* **7D**, 153 (1983).
- [49] J. Mandelbrot, *Fluid Mech.*, **62**, 331 (1974).
- [50] U. Frisch and G. Parisi, in *Turbulence and Predictability in Geophysical Fluid Dynamics and Climate Research*, edited by M. Ghil, R. Benzi and G. Parisi (North-Holland, Amsterdam, 1985) p.84.
- [51] T. C. Halsey, M. H. Jensen, L. P. Kadanoff, I. Procaccia and B. I. Shraiman, *Phys. Rev. A* **33**, 1141 (1986).
- [52] A. B. Chhabra and R. V. Jensen, *Phys. Rev. Lett.* **62**, 1327 (1989).
- [53] J. Kaplan and J. Yorke, in *Functional Differential Equations and the Approximation of Fixed Points*, Vol. 730 of *Lecture Notes in Mathematics*, eds.: H. O. Peitgen and H. O. Walther (Springer-Verlag, Berlin, 1980).
- [54] R. Preston, *The Mountains of Pi*, *The New Yorker*, Mar. 2, 1992, p. 36.
- [55] V. I. Arnold, *Mathematical methods of classical mechanics* (Springer, Berlin, 1989).
- [56] D. J. Evans, E. G. D. Cohen and G. P. Morriss, *Phys. Rev. A* **42**, 5990 (1990).
- [57] B. L. Holian, W. G. Hoover and H. A. Posch, *Phys. Rev. Lett.* **59**, 10 (1987).

- [58] J. L. Lebowitz, first round-table remarks in *Simulation of Complex Hydrodynamic Phenomena*, edited by M. Mareschal, NATO-ASI in Alghero, Sardinia (Plenum, New York, 1992).
- [59] S. Goldstein, C. Kipnis and N. Ianiro, *J. Stat. Phys.* **41**, 915 (1985).
- [60] S. Goldstein, J. L. Lebowitz and E. Presutti, *Colloquia Math. Soc. Janos Bolyai* **27**, *Random fields* (Esztergom, Hungary, 1981).
- [61] E. T. Jaynes, *Papers on Probability, Statistics and Statistical Physics*, edited by R. D. Rosenkrantz (Kluwer, Dordrecht, 1989).
- [62] D. N. Zubarev, *Nonequilibrium Statistical Thermodynamics*, (Consultants bureau, New York, 1974).
- [63] W. G. Hoover, *J. Stat. Phys.* **42**, 587 (1986).
- [64] H. A. Posch, H. Narnhofer and W. Thirring, *J. Stat. Phys.* **65**, 555 (1991).
- [65] W. Pusz and S. L. Woronowicz, *Commun. Math. Phys.* **58**, 273 (1978).
- [66] A. Lenard, *J. Stat. Phys.* **19**, 575 (1978).